HHS Public Access

Author manuscript

Science. Author manuscript; available in PMC 2018 December 28.

Published in final edited form as:

Science. 2018 April 20; 360(6386): 323–327. doi:10.1126/science.aar7924.

Structure of a prehandover mammalian ribosomal SRP·SRP receptor targeting complex

Kan Kobayashi[#1], **Ahmad Jomaa**[#1], **Jae Ho Lee**[2], **Sowmya Chandrasekar**[2], **Daniel Boehringer**[1], **Shu-ou Shan**[2], and **Nenad Ban**[1,†]

[1]Department of Biology, Institute of Molecular Biology and Biophysics, ETH Zurich, Otto-Stern-Weg 5, Zurich CH-8093, Switzerland. [2]Division of Chemistry and Chemical Engineering, California Institute of Technology, Pasadena, CA 91125, USA.

[#] These authors contributed equally to this work.

Abstract

Signal recognition particle (SRP) targets proteins to the endoplasmic reticulum (ER). SRP recognizes the ribosome synthesizing a signal sequence and delivers it to the SRP receptor (SR) on the ER membrane followed by the transfer of the signal sequence to the translocon. Here, we present the cryo–electron microscopy structure of the mammalian translating ribosome in complex with SRP and SR in a conformation preceding signal sequence handover. The structure visualizes all eukaryotic-specific SRP and SR proteins and reveals their roles in stabilizing this conformation by forming a large protein assembly at the distal site of SRP RNA. We provide biochemical evidence that the guanosine triphosphate hydrolysis of SRP·SR is delayed at this stage, possibly to provide a time window for signal sequence handover to the translocon.

In eukaryotes, nascent secretory and membrane proteins are cotranslationally targeted to the endoplasmic reticulum (ER) membrane by the universally conserved signal recognition particle (SRP) and its receptor (SR) (1–3). SRP recognizes the N-terminal signal sequence of the nascent chain on ribosomes synthesizing membrane or secretory proteins (4–6). Subsequently, through interactions with the membrane-anchored SR, the ribosome–nascent chain complex (RNC) is delivered to the Sec translocon (Sec61p) on the ER membrane (7, 8).

[†]**Corresponding author.** ban@mol.biol.ethz.ch.

Author contributions: K.K., A.J., S.-o.S., and N.B. designed the experimental strategy. K.K. prepared samples and grids for the cryo-EM analysis. K.K., A.J., and D.B. collected cryo-EM data. K.K. and A.J. processed data, built the structure model, and refined it. J.H.L. and S.C. prepared samples for the functional assays and performed them. K.K. and A.J. wrote the initial draft of the manuscript, and all authors contributed to the final version.

Competing interests: None declared.

Data and materials availability: The atomic coordinates have been deposited in the Protein Data Bank (PDB ID: 6FRK). The cryo-EM density map has been deposited in Electron Microscopy Data Bank (EMD-4300).

SUPPLEMENTARY MATERIALS

www.sciencemag.org/content/360/6386/323/suppl/DC1

The eukaryotic SRP targeting machineries are considerably more complex than their bacterial counterparts (9,10). The eukaryotic SRP contains a larger SRP RNA (7SL for mammals) composed of S and Alu domains (11) and six eukaryotic proteins (SRP9, SRP14, SRP19, SRP54, SRP68, and SRP72) (1), out of which only SRP54 is universally conserved. SRP54 binds the ribosomal tunnel exit and the signal sequence through its NG (12) and M domains (13), respectively. Eukaryotic SR is a heterodimer of SRα and eukaryotic-specific SRβ integrated into the ER membrane (14,15). SRα contains a universally conserved NG domain, a flexible linker, and a eukaryotic-specific SRX domain that complexes with SRβ (16). The NG domains of SRP54 and SRα interact in a guanosine triphosphate (GTP)–dependent manner to form the NG heterodimer (17,18), thus delivering translating ribosomes to the ER.

By analogy to the bacterial SRP pathway (19,20), it is assumed that the GTP-bound NG heterodimer of SRP·SR relocates from the ribosomal tunnel exit to the distal region of the SRP RNA where GTP is hydrolyzed. This conformational change might be necessary for the attachment and signal sequence handover to the Sec61p translocon (18, 21). Both SRP68 and SRP72 proteins are likely to be involved in distal site interactions and GTP hydrolysis based on their positions on the SRP RNA (18, 22) and because chemical modification of these proteins severely represses membrane targeting activity (23). Previous studies also suggested roles of the eukaryotic-specific SR components SRX and SRβ in guanosine triphosphatase (GTPase) regulation (24) and signal sequence handover to the Sec61p translocon (25, 26), respectively. However, the implications of the mechanistic and architectural differences between the bacterial and eukaryotic SRP systems have been difficult to rationalize. We set out to obtain structural information on the complete eukaryotic protein targeting complex on the translating ribosome.

The mammalian SRP·SR·RNC targeting complex was assembled in the presence of 5′-guanylyl imidodiphosphate (GMPPNP), and its structure was determined using single-particle cryo–electron microscopy (cryo-EM) at 3.7-Å resolution on average (Fig. 1 and figs. S1 and S2). The densities of SRP and SR were resolved around 4.5- to 10-Å resolution (fig. S2, C and D), and the SRP RNA is visualized in its entirety (Fig. 1A and fig. S2C). At the Alu domain, the SRP RNA and SRP9/14 contact ribosomal subunit interface to arrest translation as previously observed (27) (fig. S3, A and B). In the S domain, the ribosomal tunnel exit has the density for the SRP54 M domain bound to the signal sequence (Fig. 1B and figs. S3, C and D, and S4A) but lacks that for its NG domain (Fig. 1, A and B), consistent with previous cryo-EM structures of the SRP·SR·RNC complex (21, 28, 29). Instead, a large density is visible at the distal region of the SRP RNA (Fig. 1A), where we can dock previously reported crystal structures of SRP and SR proteins (Fig. 1B and figs. S4 and S5) (18, 22, 30, 31). This structure reveals an architecture of the entire mammalian SRP·SR·RNC complex (Fig. 1, B and C).

Compared with the structure of the SRP·RNC complex without the receptor (27), the SRP RNA lifts away from the ribosomal tunnel exit by ~12 Å (fig. S6), which would facilitate the transfer of the signal sequence to the Sec61p translocon. At the distal site of the SRP RNA, the NG heterodimer binds to the SRP RNA at a different angle compared with its bacterial counterpart (29) (fig. S7), leading to additional contacts with the SRP RNA, the ribosome,

the SRP proteins, and SR (Fig. 2 and fig. S8, A to C). The linker between NG and M domains (GM-linker) of SRP54 connecting its NG and M domains, which forms a helix in the bacterial complex, is flexibly disposed and is not visible in the map (Fig. 1B and fig. S7). The resolution of the SRP RNA at the contact site with the NG heterodimer is ~4.5 Å (fig. S2C), resolving the phosphate backbone of the SRP RNA along with a flipped-out base stacking with Phe^{456} of the NG domain of SRα in the GTPase active site (figs. S2D and S9). The position of this flipped-out base corresponds to that of the universally conserved G232 (bacterial G83) (22, 31, 32). The interactions between the SRα NG domain and the SRP RNA, including the contacts formed by the flipped-out base and the surrounding helices of the NG domain, are similar to the interactions seen for the GTPase-activated bacterial complex (32) (figs. S8C and S9). The SRα NG domain also interacts with the SRP68 RBD (Fig. 2 and fig. S8C), whereas the extended loop of SRP68 RBD makes contact with the 28*S* ribosomal RNA (rRNA) (fig. S8D).

In the mammalian targeting complex, the NG heterodimer at the SRP RNA distal site is locked in position by extensive interactions with SRX·SRβ, which bridges the SRP68 RBD and the NG heterodimer (Figs. 1, B and C, and 2, and figs. S4, C and D, and S7). The cytosolic domain of SRβ belongs to the Ras GTPase superfamily (14) and forms a heterodimer with SRX in the GTP-bound form (33, 34). The interaction interface of SRβ to SRX has similarity to the binding site of Ras to its GTPase activator GAP-334, although SRX alone does not activate the GTPase of SRβ (30). In the structure of the targeting complex, SRα NG further extends the interaction interface of SRβ in a similar manner as observed in the structure of the Ras·GAP-334 complex (35) (fig. S10), but, in contrast to GAP-334, no elements from either SRX or the SRα NG domain are in direct contact with the SRβ-bound GTP (fig. S10). It appears that SRβ does not hydrolyze GTP even in this conformation and that GTP-bound SRβ may rather provide the eukaryotic-specific stabilizing effect on the NG heterodimer binding at the SRP RNA distal site. Thus, SRX·SRβ and SRP68 RBD form a platform to stably dock the NG heterodimer at the distal site of SRP RNA to enable signal sequence handover to the Sec61p translocon at the exposed ribosomal tunnel exit.

At the distal site of SRP RNA, the SRP72 RBD can be observed extending from the SRP RNA to the ribosome surface, where it approaches a hairpin of the ribosomal protein uL3 (fig. S4F). The C-terminal region of SRP72 RBD was proposed to form an alpha helix (C4 helix) and mediate interactions with the 28*S* rRNA (C4 contact) (fig. S11A) (22). However, in our map, it appears that the C-terminal region of the SRP72 RBD rather extends toward the SRP·SR NG heterodimer interface and interacts with the two stacking residues in the GTPase active site, G232 of the SRP RNA and Phe^{456} of SRα (Fig. 3, A and B, and figs. S9A and S11B). Thus, a eukaryotic-specific GTPase regulation mechanism may involve a protein component of the SRP (SRP72) in addition to the SRP RNA. To determine whether mutations in SRP72 affect the GTPase activity of the targeting complex, we prepared SRP variants harboring mutation or deletion in the SRP72 C-terminal region containing the C4 helix (Arg^{589}-Gln^{603} based on the human numbering) (fig. S12A). All tested SRP mutants were active in translation arrest and membrane targeting in vitro (fig. S13), indicating that they were not defective in ribosome interactions. GTPase assays of SRP·SRαβΔTM (lacking nonessential luminal and transmembrane regions of SRβ) complexes assembled with the

ribosome and signal sequence showed that, unexpectedly, all the SRP variants exhibited enhanced GTPase activity compared with wild-type SRP (Fig. 3C and fig. S14). Enhanced GTPase activity was also observed when we modified SRP RNA by mutating the flipped-out G232 into A (G232A) or by closing the SRP RNA 5f-loop (ΔΔ231, G232U) (Fig. 3D and figs. S12B and S14), and the highest GTPase activity was observed by combining the mutations on the SRP RNA and SRP72 (Fig. 3D and fig. S14). In addition, an SRX·SRβ–deletion mutant of SR (SRαΔX) also exhibited a two-fold more enhanced GTPase activity than SRαβΔTM (Fig. 3C). Thus, eukaryotic-specific interactions at the SRP RNA distal site delay GTP hydrolysis, in contrast to the bacterial system, where distal site interactions between SRP RNA and NG heterodimer stimulate GTP hydrolysis (20, 32). The delay of GTP hydrolysis by the SRP·SR NG heterodimer at the distal site of the SRP RNA may provide a eukaryotic-specific regulatory role. Interestingly, it was reported that the C-terminal region of SRP72 is cleaved during apoptosis, further supporting its possible role in regulating the targeting process (22, 36). We propose that the current structure represents a “prehandover” complex of SRP·SR at the SRP RNA distal site, which allows docking of the Sec61p translocon onto the exposed ribosomal tunnel exit. Delayed GTP hydrolysis in this state might provide a longer time window for the nascent polypeptide to engage the Sec61p translocon, which was proposed to be slow in eukaryotic systems (37), before the detachment of SRP and SR from RNC. Indeed, the mammalian Sec61p translocon reduces the GTPase activity of SRP·SR in the presence of RNC (38).

In conclusion, this study reveals the roles of eukaryotic-specific components of the SRP and SR proteins in the mammalian targeting process. This process starts by the recognition of the signal sequence by SRP at the exit of the ribosomal tunnel and formation of the SRP54·SRα NG heterodimer in the presence of GTP (Fig. 4, A and B). The NG heterodimer then relocates to the SRP RNA distal site, where it forms a large complex stabilized by interactions with the eukaryotic-specific components of the SRP and SR together with SRP RNA (Fig. 4C). At this stage, the GTP hydrolysis of the NG heterodimer is delayed to provide a time window for the signal sequence handover from SRP to the Sec61p translocon at the exit of the ribosomal tunnel.

Supplementary Material

Refer to Web version on PubMed Central for supplementary material.

ACKNOWLEDGMENTS

Cryo-EM data was collected at the Scientific Center for Optical and Electron Microscopy at the ETH Zurich (ScopeM). We thank P. Tittmann and A. Scaiola for support with data collection and C. Aylett and M. Itten for support with data processing. We also thank P. Bieri for initial help with microsome preparation and structure model building. We are grateful for M. Leibundgut for the critical comments on our structure model and manuscript.

Funding: K.K. was supported by Long-Term Fellowships from Toyobo Biotechnology Foundation and European Molecular Biology Organization (EMBO) (ALTF 660-2015). This study was supported by the Swiss National Science Foundation (SNSF) (grant number 310030B_163478), National Center of Excellence in Research (NCCR) RNA & Disease Program of the SNSF (grant number 51NF40_141735) (to N.B.), NIH grant GM107368, Gordon and Betty Moore Foundation grant GBMF2939, and a fellowship from the Weston Havens Foundation (to S.-o.S.).

REFERENCES AND NOTES

1. Walter P, Blobel G, Proc. Natl. Acad Sci. U.S.A 77, 7112–7116 (1980). [PubMed: 6938958]
2. Gilmore R, Walter P, Blobel G, J. Cell Biol 95, 470–477 (1982). [PubMed: 6292236]
3. Meyer DI, Krause E, Dobberstein B, Nature 297, 647–650 (1982). [PubMed: 7088152]
4. Chartron JW, Hunt KCL, Frydman J, Nature 536, 224–228 (2016). [PubMed: 27487213]
5. Walter P, Ibrahimi I, Blobel G, J. Cell Biol 91, 545–550 (1981). [PubMed: 7309795]
6. Krieg UC, Walter P, Johnson AE, Proc. Natl. Acad. Sci. U.S.A 83, 8604–8608 (1986). [PubMed: 3095839]
7. Simon SM, Blobel G, Cell 65, 371–380 (1991). [PubMed: 1902142]
8. Voorhees RM, Hegde RS, Curr. Opin. Cell Biol 41, 91–99 (2016). [PubMed: 27155805]
9. Nyathi Y, Wilkinson BM, Pool MR, Biochim. Biophys. Acta 1833, 2392–2402 (2013). [PubMed: 23481039]
10. Mandon EC, Trueman SF, Gilmore R, Cold Spring Harb. Perspect. Biol 5, a013342 (2013). [PubMed: 23251026]
11. Walter P, Blobel G, Nature 299, 691–698 (1982). [PubMed: 6181418]
12. Halic M et al., Nature 427, 808–814 (2004). [PubMed: 14985753]
13. Lütcke H, High S, Römisch K, Ashford AJ, Dobberstein B, EMBO J. 11, 1543–1551 (1992). [PubMed: 1314169]
14. Miller JD, Tajima S, Lauffer L, Walter P, J. Cell Biol 128, 273–282 (1995). [PubMed: 7844142]
15. Tajima S, Lauffer L, Rath VL, Walter P, J. Cell Biol 103, 1167–1178 (1986). [PubMed: 3021779]
16. Young JC et al., J. Biol. Chem 270, 15650–15657 (1995). [PubMed: 7797564]
17. Rapiejko PJ, Gilmore R, Cell 89, 703–713 (1997). [PubMed: 9182758]
18. Wild K et al., J. Mol. Biol 428, 2880–2897 (2016). [PubMed: 27241309]
19. Ataide SF et al., Science 331, 881–886 (2011). [PubMed: 21330537]
20. Shen K, Arslan S, Akopian D, Ha T, Shan SO, Nature 492, 271–275 (2012). [PubMed: 23235881]
21. Halic M et al., Science 312, 745–747 (2006). [PubMed: 16675701]
22. Becker MMM, Lapouge K, Segnitz B, Wild K, Sinning I, Nucleic Acids Res 45, 470–481 (2017). [PubMed: 27899666]
23. Siegel V, Walter P, Cell 52, 39–49 (1988). [PubMed: 2830980]
24. Mandon EC, Jiang Y, Gilmore R, J. Cell Biol 162, 575–585 (2003). [PubMed: 12913112]
25. Bacher G, Pool M, Dobberstein B, J. Cell Biol 146, 723–730 (1999). [PubMed: 10459008]
26. Fulga TA, Sinning I, Dobberstein B, Pool MR, EMBO J. 20, 2338–2347 (2001). [PubMed: 11331598]
27. Voorhees RM, Hegde RS, eLife 4, e07975 (2015).
28. Jomaa A, Boehringer D, Leibundgut M, Ban N, Nat. Commun 7, 10471 (2016). [PubMed: 26804923]
29. Jomaa A et al., Nat. Commun 8, 15470 (2017). [PubMed: 28524878]
30. Schlenker O, Hendricks A, Sinning I, Wild K, J. Biol. Chem 281, 8898–8906 (2006). [PubMed: 16439358]
31. Grotwinkel JT, Wild K, Segnitz B, Sinning I, Science 344, 101–104 (2014). [PubMed: 24700861]
32. Voigts-Hoffmann F et al., Mol. Cell 52, 643–654 (2013). [PubMed: 24211265]
33. Legate KR, Falcone D, Andrews DW, J. Biol. Chem 275, 27439–27446 (2000). [PubMed: 10859309]
34. Schwartz T, Blobel G, Cell 112, 793–803 (2003). [PubMed: 12654246]
35. Scheffzek K et al., Science 277, 333–338 (1997). [PubMed: 9219684]
36. Utz PJ et al., J. Biol. Chem 273, 35362–35370 (1998). [PubMed: 9857079]
37. Cheng Z, Gilmore R, Nat. Struct. Mol. Biol 13, 930–936 (2006). [PubMed: 16980973]
38. Bacher G, Lütcke H, Jungnickel B, Rapoport TA, Dobberstein B, Nature 381, 248–251 (1996). [PubMed: 8622769]

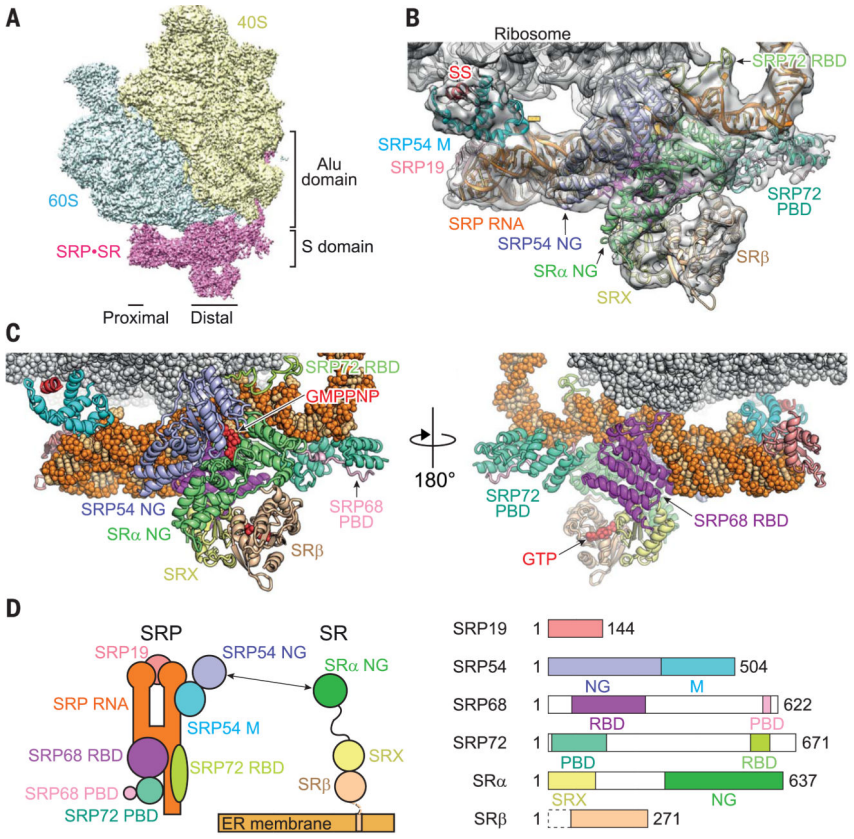

Fig. 1. Architecture of the mammalian SRP·SR·RNC complex.

(A) The cryo-EM map of SRP·SR·RNC complex low-pass filtered to 3.7-Å resolution is shown. SRP·SR and ribosomal 40S and 60S subunits are colored magenta, yellow, and light blue, respectively. **(B)** Overall structure model of SRP S domain bound to SR on RNC fitted into the map. The cryo-EM map low-pass filtered to 6-Å resolution is colored gray. Models are shown in the cartoon. The ribosome and SRP RNA are colored gray and orange, respectively. The signal sequence (SS) is colored red, and protein components of SRP and SR are colored based on their domain architectures [SRP19, salmon; SRP54 NG, light blue; SRP54 M, cyan; SRP68 RNA binding domain (RBD), magenta; SRP68 protein binding domain (PBD), light pink; SRP72 PBD, green cyan; SRP72 RBD, limon; SRα SRX, yellow; SRα NG, lime; SRβ, wheat]. (**C**) The structure model of SRP S domain and SR on the RNC from two opposite directions. The ribosome and SRP RNA are shown as spheres, and the signal sequence and protein components of SRP and SR are shown in the cartoon. Models are colored as in Fig. 1B, but bases of SRP RNA are colored light orange. The two GMPPNP molecules bound to NG heterodimer and a GTP molecule bound to SRβ are shown as red spheres. The positions of these molecules are based on the previous crystal structures (PDB ID: 5L3Q and 2FH5) (18, 30). (**D**) Schematic diagram of SRP and SR (left) and the domain architecture of SRP and SR proteins (right). SRP and SR components are colored as in Fig. 1B. The interaction between NG domains of SRP54 and SRα is depicted in an arrow. In the right panel, regions shown as blank boxes are not modeled in the structure. The N terminus of SRβ, shown as a blank box with a dashed line, depicts the luminal and transmembrane regions and is not included in the purified construct of SR.

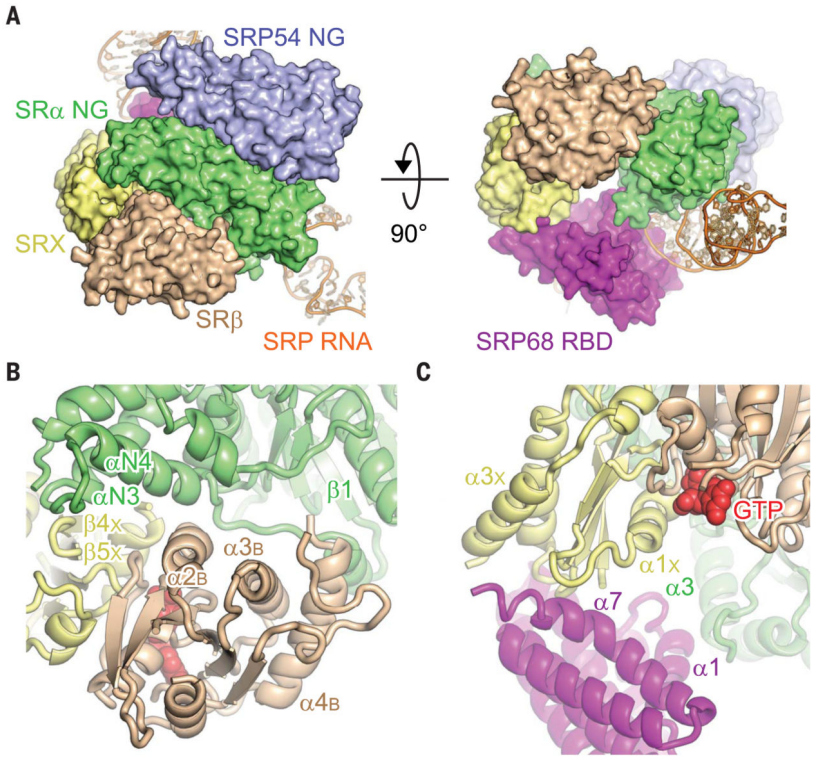

Fig. 2. Assembly of the NG heterodimer, SRP68 RBD, and SRX·SRβ at the SRP RNA distal site.

(**A**) Surface representation of the NG heterodimer, SRP68 RBD, SRX·SRβ at the SRP RNA distal site from two perpendicular directions. SRP RNA is shown in the cartoon. Other components are omitted for clarity. Models are colored as in Fig. 1B. (**B** and **C**) The interaction between NG heterodimer, SRP68 RBD, and SRX·SRβ. Proteins are shown in the cartoon and colored as in Fig. 1B. A GTP molecule bound to SRβ is also shown as in Fig. 1C. Secondary structure elements of proteins are labeled.

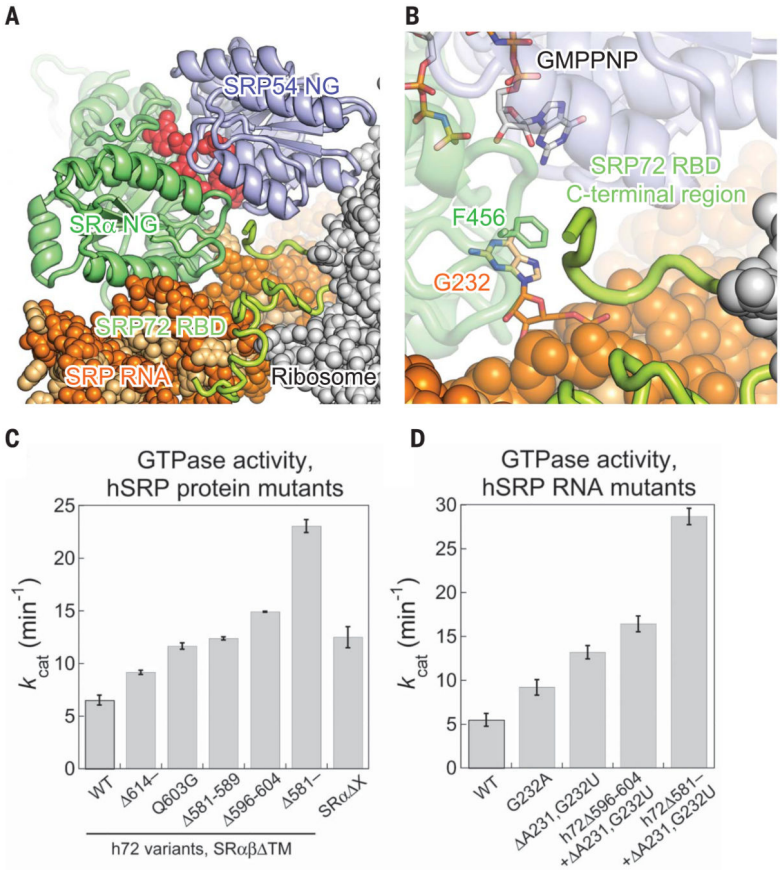

Fig. 3. The GTPase regulation of mammalian SRP·SR on RNC.

(**A**) The structure model of the NG heterodimer GTPase active site shown as in Fig. 1C. Components other than the NG heterodimer, SRP RNA, SRP72 RBD, and ribosome are omitted for clarity. (**B**) Close-up view of (A). Two GMPPNP molecules, Phe^{456} of SRα NG, and flipped-out G232 of SRP RNA are shown in the stick model. (**C**) GTPase rate constants of the SRP·SR complex formed by wild-type human SRP (hSRP) with SRαβΔTM, SRPs bearing indicated SRP72 (h72) mutations with SRαβΔTM, and wild-type SRP with SRαΔX. All measurements were carried out with SRP54 fused to a model signal sequence and with the 80S ribosome present. The values of k_{cat} were derived using analysis as shown in fig. S14. See the supplementary materials for details. (**D**) GTPase rate constants of the SRP·SR complex containing wild-type human SRP and SRPs bearing indicated SRP RNA mutations. The last two columns show the GTPase rate constants with SRPs containing mutations in both SRP72 (h72) and SRP RNA. All measurements used SRαβΔTM and were carried out with SRP54 fused to a model signal sequence and with the 80S ribosome present. The values of k_{cat} were derived using analysis as shown in fig. S14. Data were reported as mean ± SD, with n = 3 to 6 in (C) and (D).

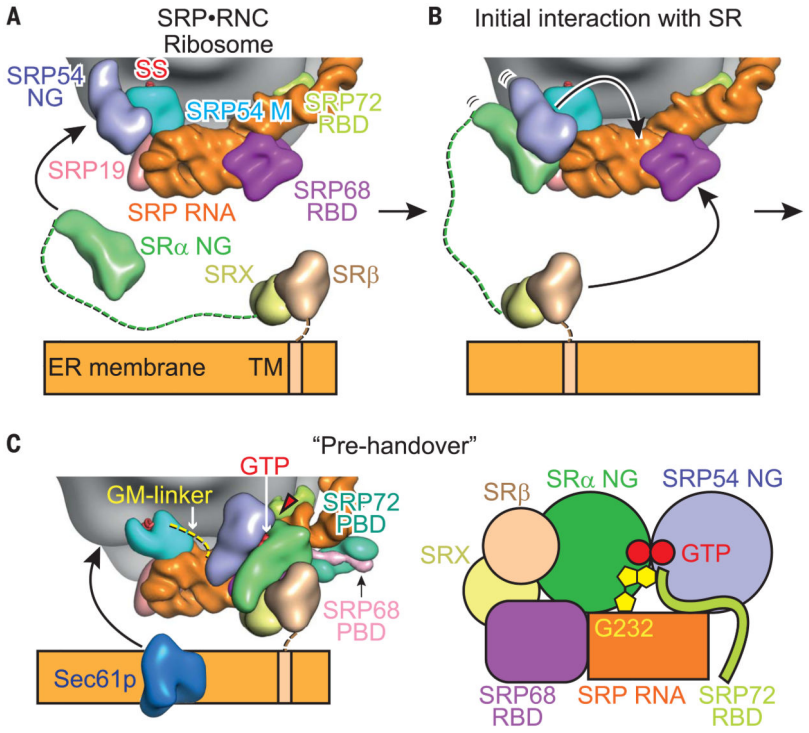

Fig. 4. Schematic diagram of the mammalian targeting system.

(**A**) In the SRP·RNC complex, the SRP54 NG domain occupies the ribosomal tunnel exit. SR is anchored to the ER membrane through the transmembrane helix (TM) of SRβ, whose cytosolic domain binds the SRX domain of SRα connected to the NG domain through the long linker. (**B**) The SRP54 NG domain initially binds SRα at the ribosomal tunnel exit, forming the NG heterodimer in the presence of GTP, which then relocates to the distal site of SRP RNA. (**C**) At the distal site of SRP RNA, SRX-SRβ together with SRP68 RBD accommodates the NG heterodimer. The GTPase active site of the NG heterodimer is pointed by the red triangle (left panel). The schematic diagram of the GTPase active site conformation is shown in the right panel. At this stage, the GTP hydrolysis is delayed by SRX·SRβ, SRP72 RBD, and SRP RNA, possibly to keep RNC on the membrane with its tunnel exit exposed for the handover of the signal sequence from SRP to the Sec61p translocon.